Journal of Engineering Mechanics and Machinery (2026)
Clausius Scientific Press, Canada

DOI: 10.23977/jemm.2026.110104
ISSN 2371-9133 Vol. 11 Num. 1

Research on the Impact of Optimized Design of Blades on Aerodynamic Performance

Zeyuan Li*, Zhiguo Shi, Weiguang Zhu

College of Mechanical Engineering, Inner Mongolia University of Technology, Hohhot, China
**Corresponding Author*

Keywords: Optimization design; Blade; Pneumatic performance; Numerical simulation

Abstract: To optimize the aerodynamic characteristics of a certain S-shaped airfoil horizontal-axis wind turbine independent intellectual property rights of a certain research group, this paper performs blade shape parameter optimization based on Wilson and Glauert design theory. This study focuses on the aerodynamic performance of both the optimized blade design and the research group's baseline blade. Utilizing the flow field analysis module of ANSYS, we investigated the rotor's torque, power, and power coefficient at six fixed wind speeds. Furthermore, the pressure distribution, pressure coefficient, and velocity streamlines around the airfoil were analyzed at various angles of attack. We can see that the new wind turbines have a higher torque by 10.70% than the original wind turbines' torque, the new wind turbines also have more power than the original wind turbines by 4.2%. At the tip speed ratio close to 5, the new wind turbine and the old wind turbine both have the largest power coefficient. When the wind speed is 8m/s and 10m/s, the newly built wind turbine wind energy coefficient is 3.9% and 2.24% greater than the old wind turbine. The curvature of the airfoil is increased, and the maximum value of the lift coefficient is also increased, so the tangential induced velocity is decreased, the turbulent diffusion on the suction side of the blade is decreased, and the energy loss of the pulsation of the airflow is reduced. Through the optimization of the new blade, it is possible to delay the separation of the boundary layer, to improve the aerodynamic performance parameters such as power and torque, and can be applied to the optimization design of horizontal-axis wind turbine blades.

1. Introduction

Recently, many studies have been done to make turbine blades more aerodynamic-especially wind and steam turbines-by using different bio-inspired and structural and flow-control based optimizations. A growing body of literature demonstrates that modifications to blade geometry, especially at critical regions such as the leading and trailing edges, can significantly improve lift-to-drag ratios, delay flow separation, and suppress dynamic stall. For instance, Zha et al. [1] investigated owl-inspired trailing-edge serrations and reported notable noise reduction and aerodynamic efficiency gains. Similarly, leading-edge protuberances or tubercles, inspired by humpback whale flippers, have been shown by Zhang et al. [2] and Hu et al. [3] to enhance performance under off-design conditions by promoting vortex generation that energizes the boundary layer. Such optimization principles extend beyond wind energy to other turbomachinery applications as well [4]. Complementary studies

by Zou et al. [5] explored wavy leading edges combined with zero-net-mass-flux jets for vertical-axis wind turbines, achieving effective dynamic stall control.

Beyond biomimicry, active and passive flow control techniques have also attracted attention. Salimipour and Yazdani [6] applied a moving surface mechanism to offshore wind turbine blades, while Hai et al. [7] examined multistage circulation control to manipulate blade loading and separation. Vortex generators under rough-wall conditions were validated by Yang et al. [8] as effective in recovering performance losses due to surface degradation. Additionally, cavity shape optimization [9] and leading-edge slats [10,11] have been proposed to re-energize airflow and maintain attached flow over the suction side. Furthermore, comprehensive optimization strategies for horizontal axis wind turbines have been demonstrated to significantly enhance aerodynamic efficiency and power output [3, 21].

Concurrently, computational and surrogate-model-driven design frameworks have accelerated blade optimization. Qianget al.[12] combined structral and aerodynamic goals with using a surrogate model. Su et al.[13] made a cooperation optimization algorithm for airfoil design using the numerial test on both how flutter is reduced and how it's aerodynamically efficient. More parametric work on geometric deviations [14], winglet configurations [15], and adaptive blades for vats [16]. Advanced numerical techniques, such as Detached Eddy Simulation (DES), have also been employed to accurately predict flow separation and optimize passive flow control mechanisms [22]. Modern blade design is a multi-disciplinary endeavor.

Moreover, erosion and operational wear-especially on offshore blades-have prompted investigations into performance recovery methods. Zhang et al. [17] analyzed mitigation strategies for leading-edge erosion, highlighting the importance of durability-aware design. In steam turbines, Fan et al. [18,19] and Wu et al. [20] demonstrated that biomimetic blade designs can also enhance internal flow efficiency and reduce losses in high-speed stages.

Collectively, these studies illustrate a paradigm shift toward integrated, multi-objective, and bio-inspired approaches in blade design, where aerodynamic performance is no longer optimized in isolation but in conjunction with structural integrity, manufacturability, environmental resilience, and operational longevity.

2. Blade Design and Computational Domain Division

2.1 Blade Optimization Design

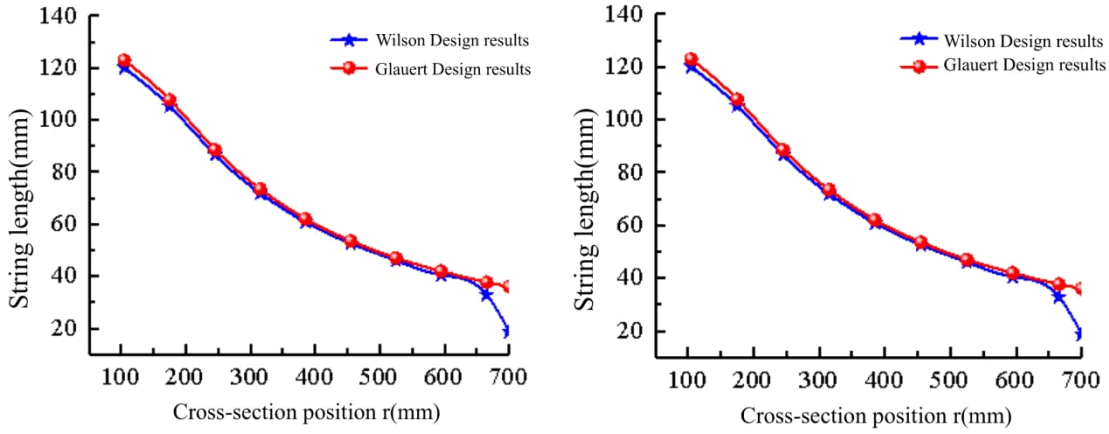

a. String length b. Twist the corner

Figure 1: Comparison chart of results

In this paper, a small wind turbine blade based on Wilson, Glauert. The objective is to obtain the

optimal chord length, twist angle, and blade performance. According to the two types of design methods and the initial blade design parameters, the rule is that the chord length and twist angle gradually decrease along the span direction of the blade, and then use Matlab programming to calculate the blade parameters. As shown in Figure 1, the calculated results are compared.

2.2 Computational domain physical model

Wind Turbine Numerical Simulation uses the actual size method, as shown in Figure 2. In the calculation area of the model, there are mainly two areas. One is rotating part where the rotor is. And other is the non - rotating part around it. The connection between the two areas is done through slip grids that can provide data information exchange and transmission. Calculation area like in the picture. Calculation region is the part of the rotating area in the rotor, and the rotor size is 1.4m, and the rotating part is a cylinder, the cylinder diameter is 1.45m. Upstream boundry of incoming flow at top end of the front of rotor is 1m apart from the central point of rotor's rotation. Downstream boundry of incoming flow 5m from the center point of rotating the rotor. Diameter of stationary flow field domain is 5m and there is an interface only between stationary flow field domain and rotating domain.

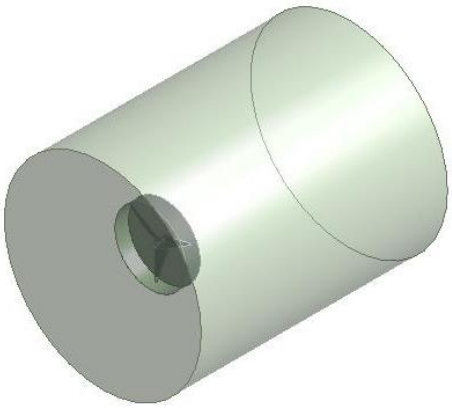

a. Computational domain physical model

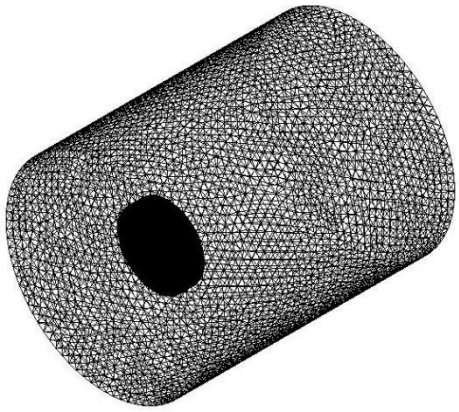

b. Computational domain grid division

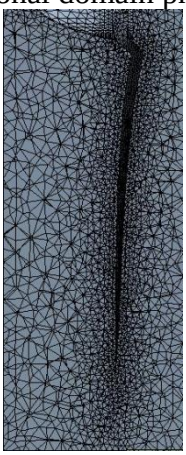

c. Grid near the blade

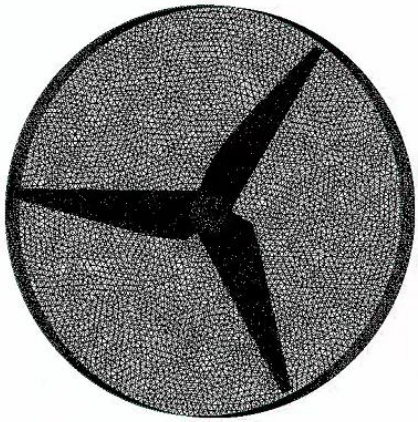

d. Mesh division in the rotating domain

Figure 2: Computational domain model

2.3 Boundary Condition Settings

Inflow condition setting: Set the wind speed as the wind speed in the wind tunnel experiment, and take the normal inlet calculation domain boundary conditions; Outlet condition setting: The outlet is set as the infinite distance behind the wind turbine. Due to infinite distance energy loss, the pressure

is close to 0 Pa; Static domain wall: According to the actual wind tunnel model, the static domain wall can be set as a no-slip wall (No Slip Wall); The interface between the rotating domain and the static domain is set as the internal interface (interface-inner) and the external interface (interface-outer); Wind turbine wall conditions: no slip wall (No Slip Wall); Turbulent model: Choose Turbulent model as Shear Stress Transport model. According to the equation $k-\omega$, the shear stress transmission. SST model is that it can analyze the shear stress of gas on the object structure.

3. Airfoil Aerodynamic Performance Analysis

3.1 Pressure Distribution

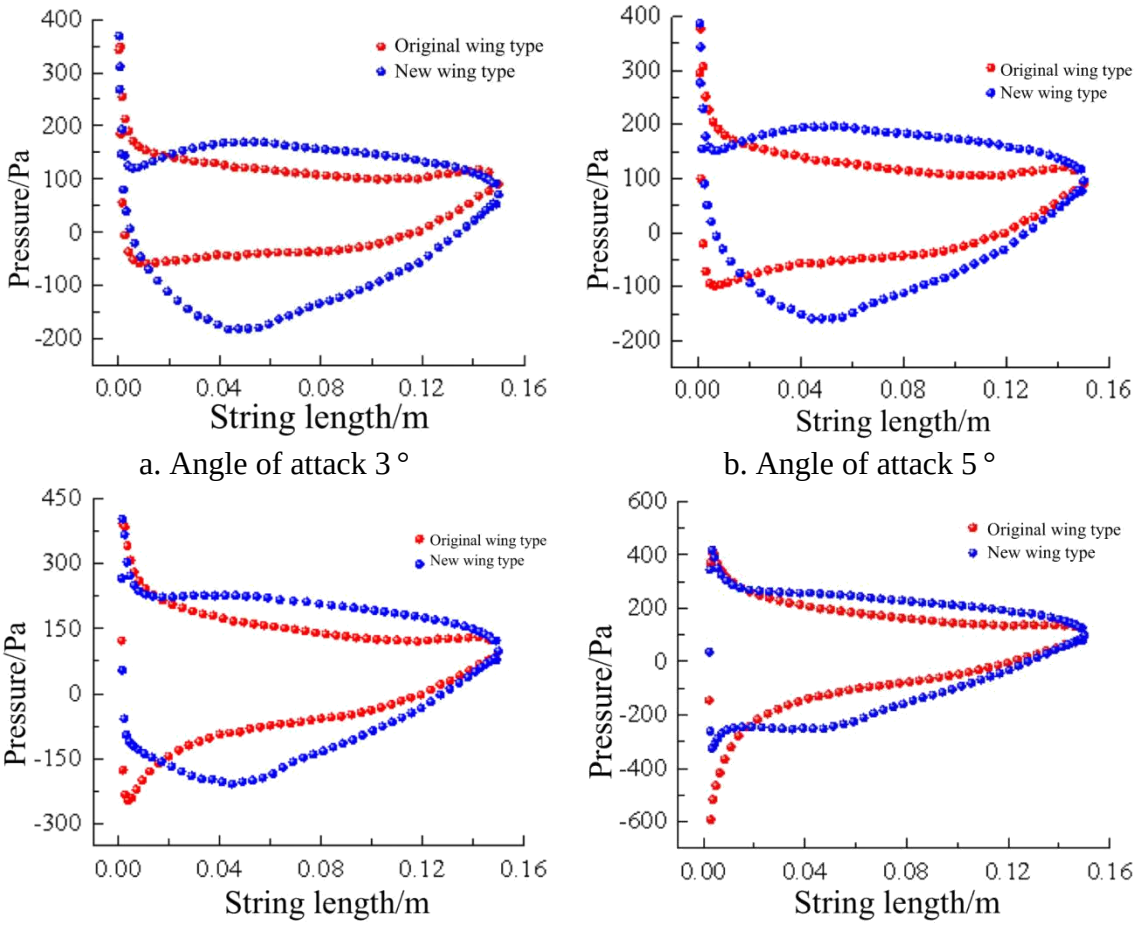

a. Angle of attack 3 °

b. Angle of attack 5 °

c. Angle of attack 7 °

d. Angle of attack 10 °

Figure 3: Pressure distribution

As we can see from Figure 3, when the wind speed is 10 m/s, the pressure and pressure coefficient analysis is carried out when the attack angle is 3 °, 5 °, 7 °, and 10 °. The top curve is the pressure distribution on the lower side, and the bottom curve is the pressure distribution on the upper side. From the figure we can see that the pressure coefficient on the upper side is much lower than that on the lower side, this is lift. The pressure difference in the pressure at the leading edge position is greater between the two airfoils. When the attack angle is 3 °-10 °, there is a sudden change in the pressure value on the lower surface at a position 0.01m away from the leading edge, and after the sudden change, the rate of pressure value change is gradually reduced. The new airfoil's pressure value is higher than the old airfoil's. For the upper surface, the pressure value of the original airfoil has a

sudden change at a distance of 0.01m from the leading edge, whereas the pressure value of the new airfoil has a sudden change around 0.05m from the leading edge, and then gradually increases. The pressure difference between the upper and lower surfaces at the beginning of the leading edge of the original airfoil is slightly higher than that of the new airfoil. The position of the leading edge gets closer and closer to the trailing edge; accordingly, the pressure on the pressure surface of the new airfoil would be larger than on the original airfoil. The pressure and pressure coefficient both decrease from the leading edge to the trailing edge. The negative pressure on the suction surface of the newly modified airfoil is obviously lower than that of the old airfoil, and the maximum positive and negative pressure happen on the pressure surface and suction surface positions at the leading edge.

3.2 Pressure Map

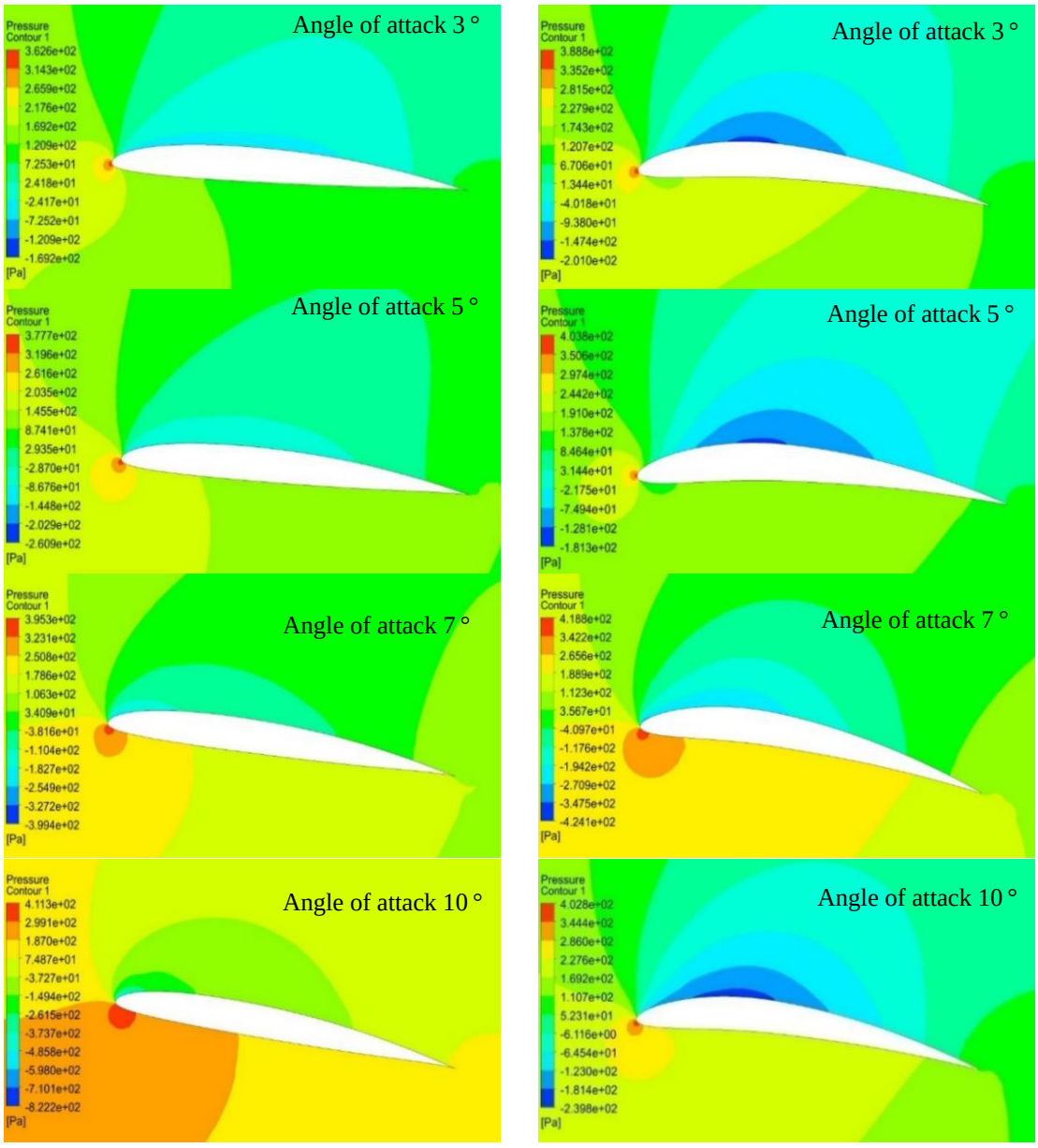

a. Original airfoil b. New airfoil

Figure 4: Pressure nephogram distribution

From the pressure map of the airfoil in Figure 4, it can be found that the suction surface of the

airfoil has a negative pressure area, and at the same time, a positive pressure area is also formed on the lower surface. And this is why it makes lift. Within the 3 ° to 10 °, with the increase of angle of attack, some changes in the negative pressure area on the suction surface can be seen. The pressure value becomes less. From the change of the pressure map we can see that the decreasing trend is quite steady. It is found by comparing the pressure map with the same angle of attack that the negative pressure area on the suction side of the new airfoil is larger than that of the original airfoil, and the pressure value is lower than that of the original airfoil.

4. Aerodynamic Performance Analysis of the Wind Turbine

4.1 Experimental Testing

This experiment was carried out in the B1/K2 type wind tunnel opening part of the Key Laboratory of Wind Energy and Solar Energy Utilization Technology of MOE at Inner Mongolia University of Technology. The open-circuit, low-speed wind tunnel was calibrated. A 400W Permanent Magnet Synchronous Generator was mounted on the wind Turbine. The operating conditions of the Wind Turbine were regulated and observed with a condition adjustment monitoring system. This system mainly contains an electronic load box and a power analyzer. The electronic load box regulates the load and thus changes the rotor's rotational speed, and the power analyzer will monitor in real time the rotor speed as well as the generated power of the wind turbine. The surface of the wooden blades is covered with fiberglass, and the hub is connected by flanges. An intelligent acquisition module was used to measure and record physical quantities such as wind turbine speed, shaft power, voltage, current, and resistance. Main experimental equipment and test blades can be seen in Figure 5. In this experiment, an aerodynamic efficiency test of the original blades was carried out and compared with the results of numerical simulation to verify the reliability of the simulation.

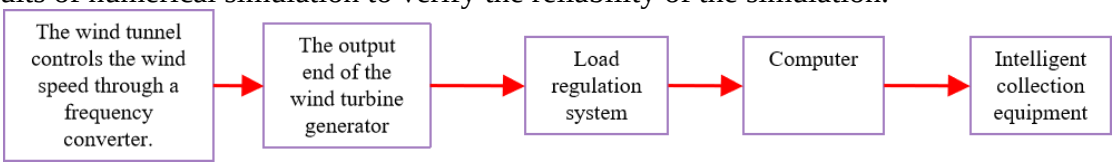

a: Diagram illustrating the principle of the experimental equipment

b: Experimental wind tunnel

c: Wind speed meter

d: Power Analyzer

e: Load Box

f: Test blade

g: Wind tunnel experiment

Figure 5: Experimental equipments and blade

4.2 Comparative Analysis of Power and Torque at Various Wind Speeds

Wind turbine's power, torque, are very important parameter, also is two parameters represent the aerodynamic's ability, also a basis to judge wind power machine aerodynamic's ability. The wind turbine determines how much torque there will be, which also determines how much power will be output by the machine. As shown in Figure 6, the new wind turbine has a power that is 4.2% greater than the old wind turbine. Because the lift of the blade airfoil of the new wind turbine has increased and the resistance has decreased compared to the old wind turbine. As can be seen from Figure 7, the torque of the new wind turbine is 16.70% higher than that of the original wind turbine at different wind speeds.[23] Power parameters can be derived from formulas for power and torque. Within a certain range of angle of attack, it can catch more wind energy. Improvement in wind energy utilization rate will increase the torque and increase the power to some extent. The difference between the numerical simulation calculation value and the experimental value of the original wind turbine is less than 10%, which proves the reliability of the numerical simulation calculation.

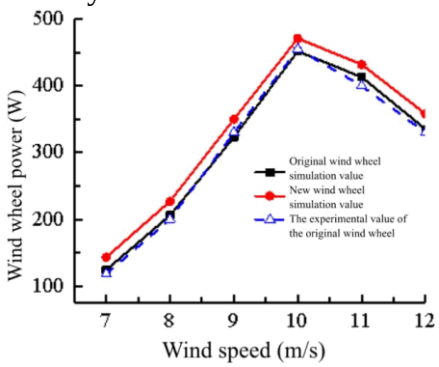

Figure 6: Rotor power

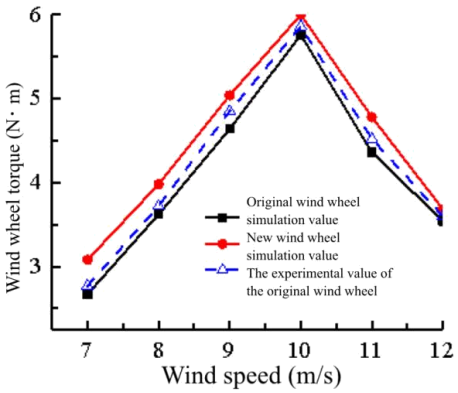

Figure 7: Rotor torque

4.3 Comparative Analysis of Power Coefficient and Torque at Different Tip Speed Ratios

The wind turbine's power coefficient's trend with different tip speed ratios at two wind speeds is shown in Figure 8. From the figure we can see that within the 3-7 range of the tip speed ratio, the power coefficient of the new wind turbine and the old wind turbine are the same. The newly designed wind turbine's power coefficient is slightly greater than that of the old wind turbine. At design tip speed ratio of 5 both new and old wind turbines have their maximum power coefficient. At a wind speed of 8m/s, the new wind turbine is about 3.9% better than the original wind turbine with a Wind Power Coefficient. At a wind speed of 10m/s, the new wind turbine is roughly 2.24% more efficient than the original wind turbine with a Wind Power Coefficient. Because when the design tip speed ratio is 5, the lift-to-drag ratio is the largest, and the power coefficient is also the largest at this time. Resultant force perp to in-flow direction is known as the lift, and that in the direction same as in-flow direction is known as the drag. When the incoming flow passes the surface of the blades, the flow goes backward from the leading edge to the trailing edge. The blade bend will create a high airflow pressure at the pressure surfaces lower section. The suction surface has more friction from the curved and smooth side which will reduce too. The laminar flow of the boundary layer is extended and the wake area is reduced, so the pressure difference between the suction surface and the pressure surface of the airfoil increases, and the lift-to-drag ratio of the airfoil increases. The inverse ratio of the lift to drag ratio, leading to a greater increase in the power coefficient than the original airfoil, thereby enhancing the wind energy utilization.[24] The power change trends of the new wind turbines and the original wind turbines are as follows. From this it can be seen that during rotation of windmill its rotating speed increases and accordingly the torque will be increasing and decreasing. At the rotational speed of 750 r/min, the wind turbine's torque at a wind speed of 8m/s is about 3.66% more and the wind turbine's torque at a wind speed of 10m/s is about 2.31% more. There are two reasons: because of the increase in the curvature of the airfoil, the maximum lift coefficient is increased, which will lead to an increase in the tangential induced velocity, so the airflow pulse turbulent diffusion on the suction surface will decrease, the energy loss of the airflow will decrease, so the torque of the wind turbine will be slightly higher than the original wind turbine at the same wind speed.

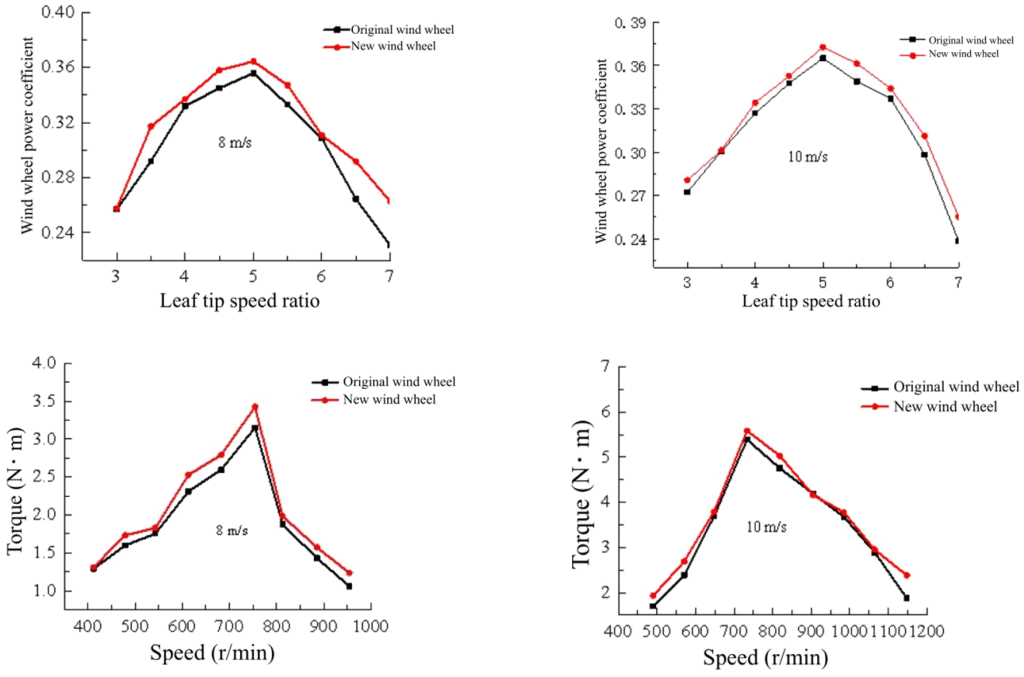

Figure 8: Comparison of aerodynamic performance

5. Conclusion and Discussion

(1) Blade Tip compared to different place it's very much different. Wilson's design also consider the blade tip loss which will lead to large change in the axial induced factor. For a finite length of blade, when a pressure difference acts on the upper and lower surfaces of the blade, there will be a lateral velocity component outwards on the lower surface of the blade. The change in the blade motion parameter is the blade energy that is consumed by the airflow to a decrease. Therefore, it will result in different blade tips. There will be a great difference in the two design methods.

(2) New wind turbine torque compared to old is 16.70% up, new power compared to old is 4.2% up. Because the increase in lift force and the decrease in drag, it is possible to catch more wind energy in a certain angle of attack. Wind energy use increasing would cause the torque to increase, which could enable some level of power increase. When the tip speed ratio is approximately 5, the new wind turbine and the original wind turbine achieve their respective maximum power coefficients. When wind speed is 8m/s, then the new wind turbine's power coefficient is roughly 3.9% greater than that of the original wind turbine, whereas at wind speed of 10m/s, the new wind turbine's power coefficient is approximately 2.24% higher than the old wind turbine's power coefficient. Because the increase in the curvature of the airfoil leads to the increase of the maximum lift coefficient, so the tangential induction velocity also increases, and then the turbulence diffusion on the suction surface of the blade reduces, the energy loss of airflow pulsation. Therefore, at the same wind speed, the new wind turbine's torque is a little larger than that of the original wind turbine.

(3) The pressure difference on the upper and lower surfaces of the starting point of the leading edge of the original airfoil is slightly larger than that of the new airfoil. The position of the leading edge will move towards the trailing edge, the pressure on the pressure surface of the new airfoil is larger than that of the old airfoil. Pressure and pressure coefficient all decrease from the leading edge to the trailing edge. The negative pressure value on the suction surface of the new airfoil is greatly reduced compared to the original airfoil, and the maximum positive and negative pressure values happen at the pressure surface and suction surface of the leading edge. The boundary layer separates at 2 °later.

References

[1] Zha R, Han Y, Du X, et al. Aerodynamic performance of blade based on owl trailingedge serrated design[J]. Journal of Physics: Conference Series,2025,3009(1):012083.DOI:10.1088/1742-6596/3009/1/012083.

[2] Yinan Z, Mingzhi Z, Mingming Z. Research on the aerodynamic performance of the wind turbine blades with leading-edge protuberances[J]. Ocean Engineering, 2023,280. DOI:10.1016/J.OCEANENG.2023.114615.

[3] Hu H, Lu B, Luo D, et al. CFD analysis of different leading edge tubercles on the aerodynamic performance of NREL phase VI wind turbine blades[J]. Energy,2025,334137721.DOI:10.1016/J.ENERGY.2025.137721.

[4] Shao W ,Feng J ,Zhang F , et al. Aerodynamic Performance Optimization of Centrifugal Fan Blade for Air System of Self-Propelled Cotton-Picking Machine[J]. Agriculture,2023,13(8):DOI:10.3390/AGRICULTURE13081579.

[5] Zou L, Zhang S, Wang J, et al. Aerodynamic performance characterization and dynamic stall control of the wavy leading-edge blades of a vertical-axis wind turbine under zero-net-mass-flux jet[J]. Energy,2026,344139801. DOI:10.1016/J.ENERGY.2025.139801.

[6] Salimipour E, Yazdani S. Improvement of aerodynamic performance of an offshore wind turbine blade by moving surface mechanism[J]. Ocean Engineering,2020,195106710.DOI:10.1016/j.oceaneng.2019.106710.

[7] Hai D, Lejie Y, Shuo C, et al. Effect of Multistage Circulation Control on Blade Aerodynamic Performance[J]. Energies,2022,15(19):7395. DOI:10.3390/EN15197395.

[8] Yang Y, Wang D, Zhang H, et al. Enhancing Aerodynamic Performance of Horizontal Axis Wind Turbine Blade Aerodynamic Performance Under Rough Wall Condition Using Vortex Generators[J]. Journal of Marine Science and Engineering,2025,13(3):397. DOI:10.3390/JMSE13030397.

[9] Energy - Renewable Energy; Researchers from Isfahan University of Technology Report on Findings in Renewable Energy (Aerodynamic Performance Improvement of Wind Turbine Blade By Cavity Shape Optimization)[J]. Energy Weekly News,2019.

[10] Energy - Wind Turbines; Jiangxi University of Science and Technology Reports Findings in Wind Turbines (Investigation of Leading-edge Slat On Aerodynamic Performance of Wind Turbine Blade)[J]. Energy & Ecology, 2020,387.
[11] Chen T ,Jiang X ,Wang H , et al. Investigation of leading-edge slat on aerodynamic performance of wind turbine blade[J]. Proceedings of the Institution of Mechanical Engineers Part C Journal of Mechanical Engineering Science,2020,235(8):095440622094188. DOI:10.1177/0954406220941883.
[12] Qiang Z, Weipao M, Qingsong L, et al. Optimized design of wind turbine airfoil aerodynamic performance and structural strength based on surrogate model[J]. Ocean Engineering,2023,289(P2): DOI:10.1016/J.OCEANENG.2023.116279.
[13] Su H, Ma J, Wang J, et al. Cooperative optimization algorithm for wind turbine airfoil design and numerical validation of blade aerodynamic and flutter performance[J]. Energy Conversion and Management,2025,333119818. DOI:10.1016/J.ENCONMAN.2025.119818.
[14] Xianjun Y ,Mingzhi L ,Guangfeng A , et al. A Coupled Effect Model of Two-Position Local Geometric Deviations on Subsonic Blade Aerodynamic Performance[J]. APPLIED SCIENCES-BASEL,2020,10(24):8976. DOI:10.3390/APP10248976.
[15] Wardhana K B, Shin B. Numerical investigation of the effect of winglet configurations with multiple cant angles on the aerodynamic performance of wind turbine blade[J]. International Journal of Sustainable Energy,2024,43(1): DOI:10.1080/14786451.2024.2403486.
[16] Longfeng H, Sheng S, Ying W. Numerical Study on Aerodynamic Performance of Different Forms of Adaptive Blades for Vertical Axis Wind Turbines[J]. Energies,2021,14(4):880. DOI:10.3390/EN14040880.
[17] Zhang Y, Zhang C, You H, et al. Analysis of performance improvement methods for offshore wind turbine blades affected by leading edge erosion[J]. Ocean Engineering,2024,310(P2):118773. DOI:10.1016/J.OCEANENG.2024.118773.
[18] Fan W, Wei J, Yanan Y, et al. Experimental and numerical investigation on aerodynamic performance of biomimetic blade in steam turbine[J].International Journal of Thermal Sciences,2023,192(PB): DOI:10.1016/J.IJTHERMALSCI.2023.108447.
[19] Fan W, An H, Wei J, et al. A biomimetic design of steam turbine blade to improve aerodynamic performance[J]. International Journal of Thermal Sciences,2022,181DOI:10.1016/J.IJTHERMALSCI.2022.107782.
[20] Wu F, Han A, Xie D, et al. Effect of the Wavy Leading Edge to Aerodynamic Performance Improvement in A Nuclear Steam Turbine Last Stage Blade[J]. ES Energy & Environment,2022,16DOI:10.30919/ESEE8C666.
[21] Rui Y, Bin J X, Ji Y. Optimal Design and Aerodynamic Performance Prediction of a Horizontal Axis Small-Scale Wind Turbine[J]. Mathematical Problems in Engineering,2022,2022. DOI:10.1155/2022/3947164.
[22] Moshfeghi M , Shams S , Ramezani M ,et al. DETACHED EDDY SIMULATION OF A PASSIVE FLOW CONTROL FOR AERODYNAMIC PERFORMANCE ENHANCEMENT AND SEPARATION REDUCTION OF A WIND TURBINE BLADE[J].Journal of Computational Fluids Engineering, 2018,23(4):24-32.
[23] E. F, T. S. Comparing the Aerodynamic Performance of Floating Offshore Wind Turbines with Optimised and Linearised Blades[J]. Journal of Physics: Conference Series,2021,2018(1):DOI:10.1088/1742-6596/2018/1/012016.
[24] Satyabrata N, Siraj A, Vilas W, et al. Effect of uniformly varying width leading-edge slots on the aerodynamic performance of wind turbine blade[J]. Materials Today: Proceedings,2023,78(P1):120-127. DOI:10.1016/J.MATPR.2022.12.194.